Asian Journal of Chemistry; Vol. 25, No. 2 (2013), 1043-1049

ASIAN JOURNAL OF CHEMISTRY

http://dx.doi.org/10.14233/ajchem.2013.13416

A Study on Some Properties of Polypropylene Based Nanocomposites Made Using Almond Shell Flour and Organoclay

AMIR LASHGARI[1,*], AYOUB ESHGHI[1,*] and MOHAMMAD FARSI[2]

[1]Department of Wood Science and Paper Technology, Karaj Branch, Islamic Azad University, Karaj, Iran
[2]Department of Wood and Paper Science and Technology, Sari Branch, Islamic Azad University, Sari, Mazandaran, Iran

*Corresponding authors: Fax+ 98 26 33203575; Tel: +98 26 33200220; E-mail: amir.lashgari@kiau.ac.ir, ayoub_eshghi@yahoo.com

(*Received*: 10 January 2012; *Accepted*: 30 August 2012) AJC-12040

The effect of nanoclay (NC) loading (0, 2.5 and 5 phr) and almond shell flour (ASF) content (30, 35 and 40 %) on the strength properties of polypropylene composites was evaluated. The amount of maleic anhydride grafted polypropylene (PP-g-MA) was constant at 2 phr for all formulations. The composite compounds were formed using a counter-rotating twin screw extruder and the specimens were made in an injection molding machine. The mechanical properties such as tensile, flexural and impact strength were measured. Results revealed the fact that when nanoclay and almond shell flour were added, the flexural and tensile modulus increased significantly, but both flexural and tensile strengths decreased slightly. The impact strength was 8 % lower besides adding 2.5 phr nanoclay, but at 5 phr nanoclay, the property was reduced to 19.6 %. At higher incorporation of both almond shell flour and nanoclay, the impact strength of composites was decreased more. The morphology of the composites containing different levels of nanoclay and almond shell flour has been examined by using X-ray diffraction (XRD) and scanning electron microscopy (SEM), respectively. XRD findings showed that with increasing nanoclay content the peak was shifted to a lower angle, which implies formation of the intercalation morphology. The mechanical properties of the composites blends made with almond shell flour were further supported by SEM micrographs.

Key Words: Nanoclay, Almond shell flour, Polypropylene, Composite, Mechanical properties, X-Ray diffraction, SEM.

INTRODUCTION

Natural fibers reinforced polymers, known as FRPs, have received a great deal of attention during the past decades[1,2]. FRPs include lignocellulosic materials, such as wood, hemp, linens, corns stalks, coconut shells, peanuts shells, almond shells, wheat and rice straws, *etc*., as fiber or filler and thermoplastic or thermoset polymers as a matrix. Although the use of natural fibers is not as popular as the use of mineral or inorganic fillers, it has several advantages over traditional fillers and reinforcing materials such as low density, flexibility during the processing with no harm to the equipment, acceptable specific strength properties and low cost on per volume basis. Despite all these advantages, there are also serious concerns. The main disadvantage of using natural fibers as fillers is their high water absorption or desorption when subjected to changes in the relative humidity of the environment and low mechanical properties, mainly, due to highly hydrophilic nature of natural fibers that causes compatibility problems with the hydrophobic polymers in composites. Various approaches are used for the improvement of mechanical properties of composites. There are two major ways to improve mechanical properties through the use of natural fillers *i.e.*, by making coupling agents and by changing its particle size. Firstly, coupling agents are used in small quantities to treat a surface so that bonding occurs between the treated surface and other surfaces. It has found polyolefin grafted with maleic anhydride, a very effective compatibilizer, reducing fiber-to-fiber interaction and thus playing an important role as a coupling agent in FRPs. Maleic anhydride grafted polyolefin such as HDPE-g-MA[3], PP-g-MA[4] and LDPE-g-MA[5] are the most common examples of reported works in the literatures. The impressive enhancement of material properties is achieved with the inclusion of submicron-size fillers such as carbon nanotubes (CNT)[6,7] and carbon nanofibers (CNF)[8], nanoclay (NC)[9], *etc*. Among different nanoparticles, nanoclay has attracted more interest as filler material and extensive researches are conducted on nanoclay as a filler material which is capable of providing reinforcement. Essential improvements of physical and mechanical properties, including tensile modulus and strength, flexural modulus and strength, thermal stability, flame resistance and barrier resistance have been observed for various thermoplastic and thermoset nanocomposites at low nanoclay content[10-14]. It is believed that such performance is due to

high cationic exchange capacity, high surface area, large aspect ratio of nanoparticles and the development of strong bonds amongst the nanoclay distributed in the polymer matrix[15]. Also there are some researches that showed reducing mechanical strength through the use of nanoclay in composites[16,17]. Commonly used nanoclays include montmorillonite, hectorite and saponite, all of which belong to the same general family of 2:1 layered or phyllo silicates. The resulting composites containing nanoclay can have several structures (Fig. 1). The structure of an intercalated nanocomposite is a tactoid with expanded interlayer spacing, but the clay galleries have a fixed interlayer spacing. Exfoliated nanocomposites are formed when the individual clay layers break off the tactoid and are either randomly dispersed in the polymer (a disordered nanocomposite) or left in an ordered array[18].

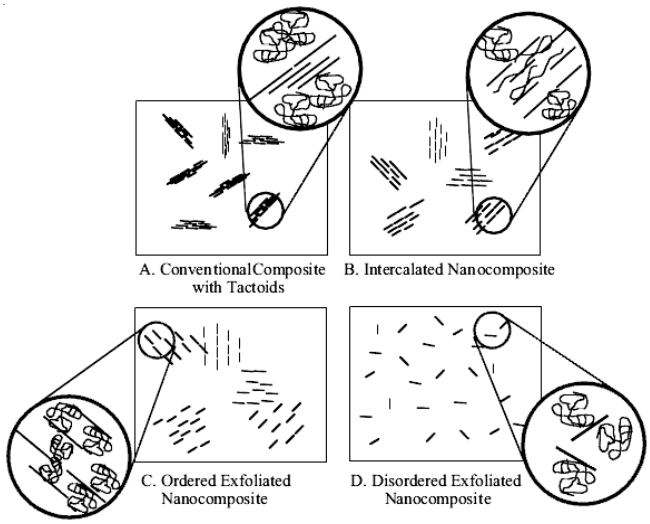

Fig. 1. Schematic of the microstructures that can develop in nanoclay-filled polymer composites: (a) a conventional composite, (b) an inter-calated nanocomposite, (c) an ordered exfoliated nanocomposites, (d) a disordered exfoliated nanocomposite

FRPs containing nanoclay could be a promising new approach to obtain better products. However, in this area few studies have been published so far that have been focused on wood-plastic composites (WPCs) containing nanoclay. In those studies, nanoclay was used as reinforcing elements and also to enhance strength properties of FRPs[9,19,20]. For example, Wang *et al.*[21] reported the exfoliation and intercalation behaviours of PE-g-MA/clay nanocomposites prepared by simple melt compounding and they concluded that exfoliation and intercalation behaviours were dependent on the PE-g-MA content and the chain length of organic modifier in the clay. Nourbakhsh and Ashori[9] also studied the effects of nanoclay 1-4 per hundred resins (phr) and coupling agents (2 and 4 phr) loaded on the physical and mechanical properties of nanocomposites. They demonstrated that when 1-3 phr nanoclay was added, the tensile properties increased significantly, but then decreased slightly as the nanoclay content increased to 4 phr and the impact strength was 6 % lower by the addition of 1 phr nanoclay, it was decreased further when the nanoclay content increased from 1-4 phr. Khanjanzadeh *et al.*[22] used organoclay as reinforcement in WPC matrix. The results indicated that the tensile and flexural properties of the composites increased with the addition of nanoclay particles up to 3 phr and decreased thereafter. However, the impact strength of the composites decreased with the incorporation of nanoclay.

A variety of natural materials has been tested to be used in FRPs. Among the various natural materials, agricultural by-products such as rice and wheat straw have attracted considerable attention in the fields of fundamental research. One of the most abundant waste materials in the west of Iran that can unlock the potentiality of these underutilized renewable materials and provide a non-food based market for the agricultural industry is almond (*Prunus duleis amygdalus*) shells. The almond shells generated in nuts processing operation are regarded as waste material and are usually burnt[23], they can probably be used as fillers in FRPs.

The main objective of this study was to prepare PP/ASF composites containing nanoclay. For this goal, the nanocomposites were manufactured and the effects of nanoclay and ASF content on composite based on polypropylene (PP) have been evaluated. The parameters such as tensile strength, flexural strength and impact properties were then measured. Since PP/ASF-organoclay nanocomposites properties can be directly affected by the intercalation/exfoliation levels in nanocomposite morphology, which depend on the raw processing material characteristics such as nanoclay type and content, compatibilizer content and matrix viscosities[24], the degree of nanoclays dispersion within the PP/ASF matrix through obtaining the distance between individual platelets of nanoclays was determined by X-ray diffraction technique. In this approach, the fractured samples have also been studied using SEM.

EXPERIMENTAL

Polypropylene (PP) supplied by Shazand (Arak) Petrochemical Co., Iran, which has a melt flow index (MFI) of 10 g/10 min and a density of 870 kg/m^3, was used as a matrix in this experiment. Maleic anhydride grafted polypropylene (PP-g-MA) as coupling agent was obtained from Solvey Co, Belgium (MFI = 64 g/10 min, 0.1 % maleic anhydride and density of 910 kg/m^3). Almond shells (AS) were collected from a nut processing plant and the grinded using Wiley mill to produce fine powder. 60-mesh almond shell flour (ASF) was used as filler. Montmorillonite modified with a dimethyl-dehydrogenated tallow, quaternary ammonium with a CEC 125 meq/100 g clay, density 1.66 g/cc and d-spacing d001 = 31.5 nm, was obtained from Southern Clay Products Co, USA, with trade name Cloisite 15 A. The polymer and nanoclay were used as received. The ASF was dried at 100 ºC in an air circulating oven for 24 h prior to use. The moisture content of the ASF was less than 1 wt. %.

Method

Composite preparation: The amount needed from each component given in Table-1 were mixed, using counter-rotating twin screw extruder (Polymer and Petrochemical Research Center of Iran) providing the mixing temperatures of 155-190 ºC in different sections of the extruder and the rotational speed of 70 rpm. The pasty compound produced was cooled to room temperature and then grinded to produce

TABLE-1
COMPOSITION OF EVALUATED FORMULATIONS

Number	Composite formula	Polypropylene (wt %)	Almond shells flour (wt %)	Nanoclay (phr*)	Coupling agent (phr)
0	100PP	100	0	0	0
1	70PP/30ASF/0NC	70	30	0	2
2	65PP/35ASF/0NC	65	35	0	2
3	60PP/40ASF/0NC	60	40	0	2
4	70PP/30ASF/2.5NC	70	30	2.5	2
5	65PP/35ASF/2.5NC	65	35	2.5	2
6	60PP/40ASF/2.5NC	60	40	2.5	2
7	70PP/30ASF/5NC	70	30	5	2
8	65PP/35ASF/5NC	65	35	5	2
9	60PP/40ASF/5NC	60	40	5	2

*Per hundred resins (the weights of nanoclay and coupling agent were calculated based on 100% weight of polymer).

suitable granules for further processing. Grinding was carried out in a laboratory mill. An injection molding machine set at 160-180 ºC temperature was used to prepare test samples. At each molding operation a complete set of specimens for different tests are produced. Finally, specimens were conditioned at a temperature of 23 ºC and relative humidity of 50 % for at least 40 h according to ASTM D618-99 before testing.

Measurements: Tensile strengths were measured according to ASTM D 638 (loading speed; 2 mm/min) and three-point flexural test were carried out according to ASTM D 790 (loading speed: 5 mm/min) using an Instron Universal Testing Machine, model 1186. Impact strength test was measured based on ASTM D 256 using SANATAM-SIT-20D impact testing machine. An X-ray diffractometer, model Philips X' Pert (Netherlands) equipped with CuK_α radiation, λ = 1.78 Å, 40 kV, 30 mA, speed: 1.2º/min and diffraction angle range 2θ = 2-12º was employed to perform XRD.

Surface morphology: Small specimens of 1 mm × 1 mm × 1 mm were cut from the strips, dried gently in an oven and coated with gold alloy. Surfaces of the samples were studied under scanning electron microscopy (model Philips XL 30) at a voltage of 17 kV.

Statistical analysis: Completely randomized block design based on 3 × 3 factorial experiments was used for statistical analysis. The analysis of variance (ANOVA) showed the significant difference between the averages at the $\alpha = 0.05$ confidence level.

RESULTS AND DISCUSSION

Dispersion behaviour of nanoclay in PP/ASF composites: XRD facilitates the understanding of the crystallographic (lamellar and intercalation) structure of nanoclay and the matrix within the nanocomposites and distribution pattern of nanoclay within the matrix. The determination of the distance between layers using Bragg's equation (eqn. 1) is one of the most important applications of the XRD[25].

$$n\lambda = 2d \sin\theta \quad (1)$$

where n is an integer, θ is the X-ray diffraction angle and λ is the wave length of the X-ray. The fine structure of the nanocomposites was analyzed using the XRD technique. A shift to lower angles of detected diffraction peak suggests an increase in interlayer spacing or gallery of the nanoclay which is referred to as intercalation[26]. Disappearance or vanishing of the nanoclays interlayer diffraction peak indicates possible exfoliation of the nanoclay platelets and broadening of the peak is considered to be the result of partial exfoliation.

The XRD patterns of the pure nanoclay and PP/ASF composites containing 2.5 and 5 phr nanoclays in the 2θ range of 2-12º spectrum are shown in Fig. 2. The peak of Closite 15A particles occurred at a 2θ value of 3.84º, with a d-spacing of 3.15 nm. With adding of nanoclay up to 5 phr to the compound, the peak related to Closite 15A was weakened and shifted to lower angles which implies formation of the intercalation morphology. However, the nanoclay was not exfoliated since the peak still obviously existed. When 2.5 phr nanoclay was compounded with PP and ASF, the position of the peak shifted to a lower angle of 2.92º, corresponding to a d-spacing of 3.49 nm. This means that the interlayer distance of nanoclay increased and the interaction of the layers should be weakened. Therefore, PP and ASF molecules could then enter the galleries of the nanoclay during the compounding step. It seems, in this study that the nanoclay could not achieve exfoliation morphology. The interlayer distance increase might result from the stronger shear during processing when ASF was introduced. As shown in Fig. 2, XRD peak of composite containing 5 phr nanoclay was present at the position of 2.94º which corresponds to a d-spacing of 3.48 nm. These data show the fact that the order of intercalation is higher for 2.5 phr of nanoclay than for the 5 phr of nanoclay concentration. However, there are no major differences between diffraction angle and d-spacing of nanoclay with 2.5 and 5.0 phr concentration.

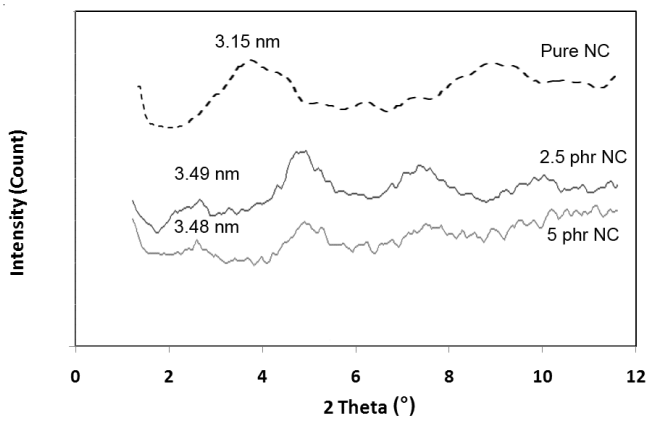

Fig. 2. XRD patterns of pure nanoclay and composites containing different loading of nanoclay

Tensile strength: The tensile strength and modulus of PP/ASF composites containing different contents of nanoclay are shown in Figs. 3 and 4, respectively. As it can be seen, the tensile strength and moduli are affected by ASF and nanoclay content. The tensile modulus of composites increases with the increase in ASF at different levels of nanoclay. The increase in tensile modulus is primarily attributed to the presence of fiber, which allowed a uniform stress distribution from continuous PP matrix to dispersed fiber phase[27]. Maximum tensile modulus of elasticity ranges from 1.19-1.68 GPa for 0 phr of nanoclay with different levels of ASF. In other words, modulus of pure PP (0.92 GPa) is enhanced at least 29.8 % when ASF is added. Compared with the lower levels of ASF, the incorporation of higher amount of ASF in the composites with different levels of nanoclay, just marginally increased the tensile modulus of elasticity and especially in the case of 2.5 phr nanoclay and 40% ASF modulus is decreased, possibly due to the higher density of the final product[28]. Jordan *et al.*[29] also stated that for most systems, the density is proportional to elastic modulus, so the region directly surrounding the inclusions will be a region of high modulus. If the particles are densely packed, then the boundary layer of polymer at the interface will comprise a large percentage of the matrix and can create a system where there is no space for a low modulus region to form. Another interesting result shown in Fig. 3 is that the tensile modulus increased with the increase of nanoclay up to 2.5 phr at the same concentration of ASF. But the modulus decreases at 30% and 35% ASF from 2.5 phr to 5 phr nanoclay. With addition of nanoclay up to 5 phr, the tensile modulus of the blends with 40% ASF significantly improved (1.75 GPa). This result is consistent with the general observation that the introduction of an nanoclay into a polymer matrix increases its tensile modulus[30]. The enhancement is easily understood because filler in nanoclay form can carry more tensile load. In general, blends with high nanoclay content exhibited better tensile modulus, but this increase has only been in composites containing 40 % ASF and 5 phr nanoclay.

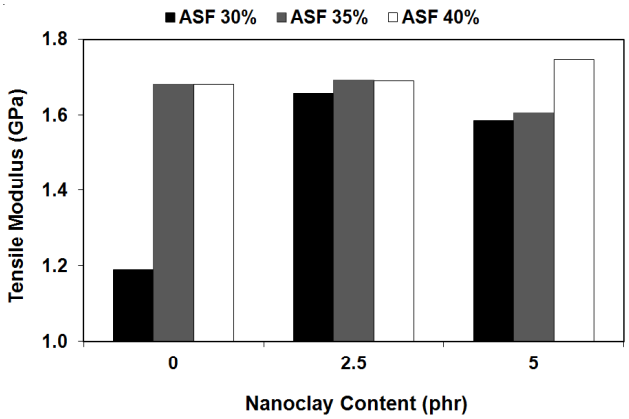

Fig. 3. Tensile modulus of PP/ASF composites containing different loading of nanoclay

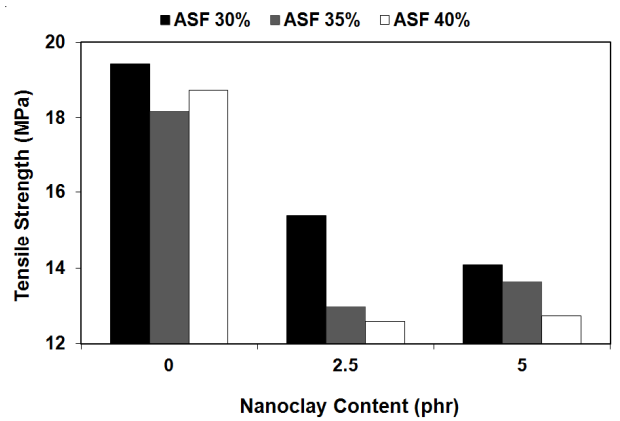

Fig. 4. Tensile strengths of PP/ASF composites containing different loading of nanoclay

As compared with PP with tensile strength of 20.15 MPa, when ASF was added, the tensile strength decreased from 19.44-18.73 MPa for 30-40 % ASF, respectively; but it is negligible (Fig. 4). The tensile strength of composites is related to interfacial strength and thus if there is weak strength in interface, the tensile strength of composites will be low. The proper interfacial strength can be achieved by incorporation of higher content of coupling agents that can be produced by exfoliation morphology. As compared with PP/ASF composites without nanoclay, with incorporation of 2.5 phr nanoclay to PP/ASF composites, the tensile strength was significantly reduced. After increasing nanoclay up to 5 phr, the tensile strength was relatively increased. This growth has been seen in composites containing 35 and 40 % ASF, respectively. Chan *et al.*[31] proposed that properties such as tensile strength and yield strength decrease in nanocomposites with polypropylene matrix due to the change in nucleation caused by the nanoparticles. The nanoparticles produce a much larger number of nucleating sites. Bensadoun *et al.*[17] also mentioned that this decrease is most probably due to the low interaction between nanoparticles dispersed in the matrix.

Flexural strength: The flexural strength and modulus of the blends are shown in Figs. 5 and 6, respectively. As it can be seen, the maximum flexural strength of PP/ASF composites ranges from 30.61-36.03 MPa, while the minimum flexural strength is approximately 26.64 MPa for pure PP. The flexural proprieties of the blends vary significantly with ASF and nanoclay loading. The flexural strength exhibits a similar trend to the tensile strength although less variation is observed in the flexural strength with different formulations than the tensile strength. The flexural strength decreases with the nanoclay increase up to 5 phr at the same content of ASF. It is probably because of the formation of clay agglomeration and the presence of voids. These agglomerates indeed act as imperfections in a composite, which can induce an untimely failure when the interfacial adhesion to the surrounding matrix is poor[32]. Also, the nanoclay is much smaller than ASF and polymer; therefore, it has been migrated into the interface of PP/ASF composite which decreased its flexural strength. It is common that the higher performance of nanocomposites is acquired by exfoliated morphology and it seems that the exfoliated morphology can be obtained using higher content of coupling agent[33-35]. The neat PP exhibited the lowest flexural modulus (0.83 GPa) compared with composites containing 30% ASF (1.08 GPa). At the constant content of ASF, the samples containing 2.5 phr nanoclay showed an increment of about 10 % in flexural modulus. The phenomenon was stronger when nanoclay content increased up to 5 phr.

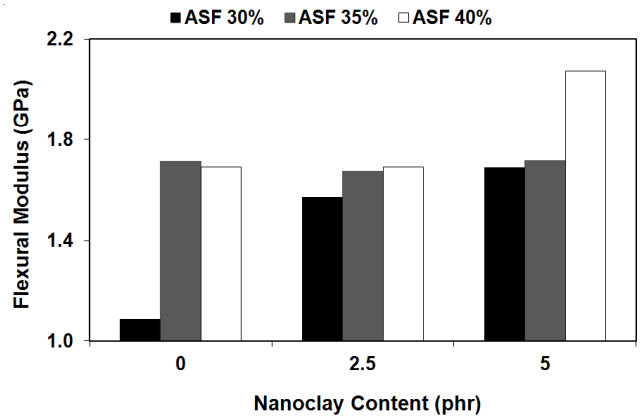

Fig. 5. Flexural modulus of PP/ASF composites containing different loading of nanoclay

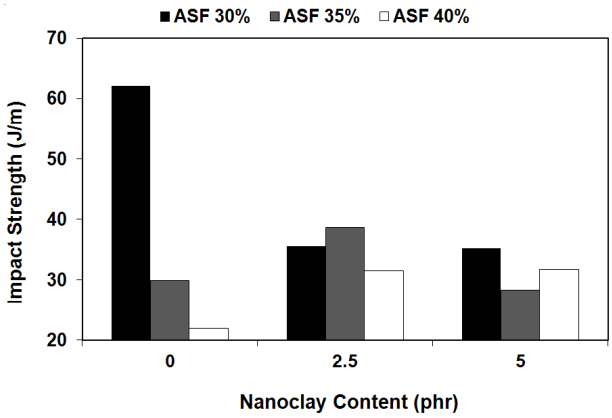

Fig. 7. Impact strengths of PP/ASF composites containing different loading of nanoclay

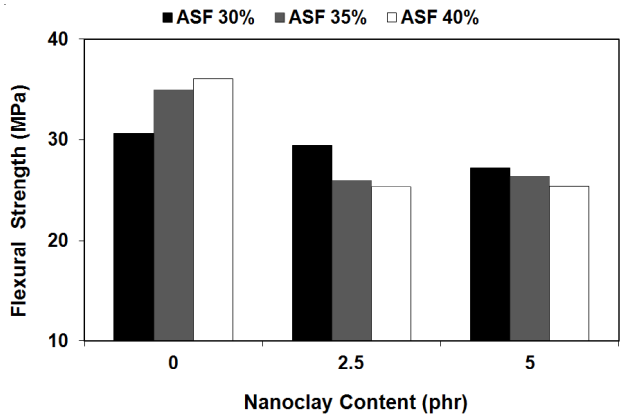

Fig. 6. Flexural strengths of PP/ASF composites containing different loading of nanoclay

The maximum flexural modulus value was found to be 2.07 GPa for composites made with 5 phr nanoclay and 40 % ASF, while flexural modulus was *ca.* 0.83 GPa for composites made with pure PP.

Impact strength: Fig. 7 represents the result of notched Izod impact strength measurements of ASF-filled polymer composites containing different levels of nanoclay. In general, the energy required crack propagation was measured with notched Izod specimen. The impact strength of nanocomposites was lower than neat PP. The nanocomposite with 40 % ASF showed the lowest impact strength (22.02 J/M) while the neat plastic exhibited the highest impact strength (94.25 J/M). The impact strength of the samples was decreased in response to increasing ASF content from 30-35 % except for the case of 35 % ASF and 2.5 phr nanoclay and then at 40 % ASF content, the impact strength was more reduced. At higher incorporation of either ASF or nanoclay, the density of the nanocomposite increased and brittle and fragile substance with lesser toughness was produced and as a consequence, the impact strength is decreased[36,37]. Also, the presence of nanoclay particles due to agglomeration of nanoparticles and the incompatibility with matrix deteriorated the bond formation between the matrix and the reinforcing component. This was expected because the presence of nanoclay in the PP matrix provides points of stress concentrations, thus providing sites for crack initiation and potential composite failure. When 2.5 phr nanoclay was used, the impact strength was slightly decreased, but at 5 phr nanoclay, the property was more reduced. These decreases were 8 and 19 %, respectively. However, significant decreases are observed for higher content of ASF.

Morphology characteristics: SEM is an effective media for the morphological investigations of the composites. Through SEM study, the distribution and compatibility between the fillers and the matrix could be observed. Fig. 8(a) shows the composite containing 30 % ASF without nanoclay. As it can be seen, the presence of numerous cavities is clearly visible in the matrix. This indicates that the level of interfacial bonding between the ASF and the PP matrix is weak and when stress is applied, it causes ASF to be pulled out from the matrix easily leaving behind gaping holes. This problem is probably related to the low level of PP-g-MA. With increasing ASF loading up to 40 %, the similar trend is also observed which is highlighted in Fig. 8(b). This figure showed more holes and cavities in the composites at the presence of 40 % ASF without nanoclay. As it can be seen in Fig. 8(c) which is related to composite including 30 % ASF and 2.5 phr nanoclay, it has been seen that a clog of nanoclay is dispersed in broken matrix. In Fig. 8(d), the composite containing 40 % ASF and 2.5 phr nanoclay shows broken and removed fibers from PP matrix because of the incompatibility between fibers and polymers and scant content of PP-g-MA. With increasing nanoclay content in composite, Fig. 8(e) shows that the ASF is pulled out from matrix and in some domains, larger particles of agglomerated ASF filler can be observed; these larger particles lead to a deterioration of the mechanical properties. Exfoliation and intercalation behaviours were severely dependent on the coupling agent content. The exfoliated morphology can be obtained using higher content of PP-g-MA. It seems, in present study, the lack of PP-g-MA could not achieve better interaction.

Conclusion

In this study, the PP/ASF composites containing nanoclay were extruded and then injection molded. The influence of nanoclay on the mechanical properties of the PP/ASF composites was investigated. The results of this study indicate that tensile and flexural strength of composites made with nanoclay and ASF decreased by about 37.7 and 25.8 %, respectively, with the addition of 2.5 phr nanoclay, but then decreased slightly as the nanoclay content increased to 5 phr. The impact

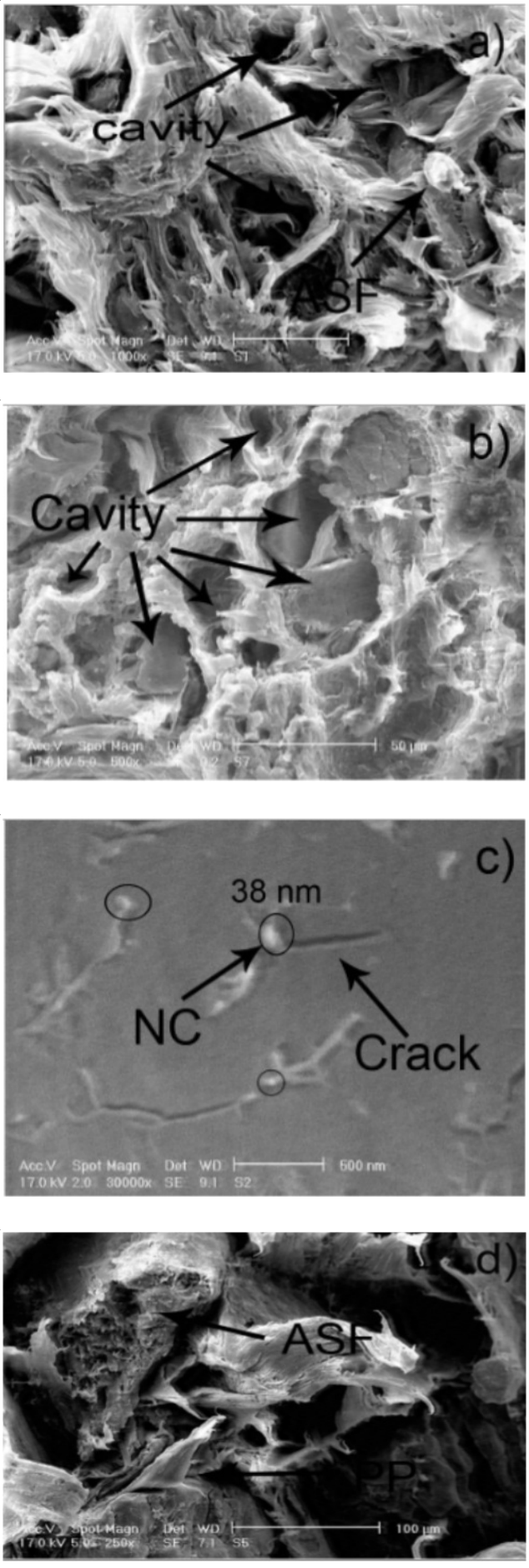

Fig. 8. SEM photomicrographs of fractured samples with formulation of (a) 70PP/30ASF/0NC, (b) 60PP/40ASF/0NC, (c) 70PP/30ASF/2.5NC (d) 65PP/35ASF/2.5NC (e) 65PP/35ASF/5NC

strength of composites significantly decreases with both incorporated fillers except for the case of PP/ASF 70/30 composite. This is reasonable because of the increased stiffness (higher modulus and lower ductility) of composites, whereas PP/ASF 70/30 composite exhibits relatively low for both modules. Both tensile and flexural moduli of nanocomposites were measured higher than PP/ASF composites. The tensile and flexural modulus of nanocomposites containing 5 phr nanoclay was increased marginally as compared with composites made up 2.5 phr nanoclay. The SEM analysis showed heterogeneous dispersions in morphologies of PP/ASF composites containing different levels of nanoclay. In some case, fibers removed from polypropylene matrix and broken, but no isolated fibrils were observed, which means that the interactions between the phases are not strong enough. Similar trend is also observed for samples containing nanoclay. The previous findings from XRD analyses demonstrated intercalation nanocomposite structures. These results have been justified for mechanical properties trends.

ACKNOWLEDGEMENTS

The authors are grateful for the support by Department of Wood and Paper Science and Technology, Islamic Azad University, Karaj Branch, Iran.

REFERENCES

1. A.K. Bledzki and J. Gassan, *Prog. Polym. Sci*., **24**, 221 (1999).
2. M. Belgacem and A. Gandini, Monomers Polymers and Composites from Renewable Resources, Elsevier, Netherlands (2008).
3. I. Polec, P.J. Hine, M.J. Bonner, I.M. Ward and D.C. Barton, *Comp. Sci. Technol*., **70**, 45 (2010).
4. M. Farsi and J. Reinf, *Plast. Comp*., **29**, 3587 (2010).
5. M. Tasdemir, H. Biltekin, G. Caneba and T. Gerald, *J. Appl. Polym. Sci*., **112**, 3095 (2009).
6. O. Faruk and L.M. Matuana, *J. Vinyl Addit. Technol*., **14**, 60 (2008).
7. H.Y. Kordkheili, S. Hiziroglu and M. Farsi, *Mater. Design*, **33**, 395 (2012).
8. J. Shi, J. Zhang, C.U. Pittman Jr., H. Toghiani and Y. Xue, *Holz. Roh. Werkst*., **66**, 313 (2008).
9. A. Nourbakhsh and A. Ashori, *J. Appl. Poly. Sci*., **112**, 1386 (2009).
10. C.M. Koo, H.T. Ham, S.O. Kim, K.H. Wang and I. Chung, *Macromolecules*, **35**, 5116 (2002).
11. Q. Wu, Y. Lei, C.M. Clemons, F. Yao, Y. Xu and K. Lian, *J. Plast. Technol*., **27**, 108 (2007).
12. Y. Lei, Q. Wu, C.M. Clemons, F. Yao and Y. Xu, *J. Appl. Polym. Sci*., **106**, 3958 (2007).

13. H. Chen, M. Wang, Y. Lin, C.M. Chan and J. Wu, *J. Appl. Polym. Sci*., **106**, 3409 (2007).
14. S.K. Samal, S. Nayak and S. Mohanty, *J. Thermoplast. Comp*., **21**, 243 (2008).
15. N. Hasegawa, H. Okamoto, M. Kato, A. Usuki and N. Sato, *Polymer*, **44**, 2933 (2003).
16. V. Selvakumar, K. Palanikumar and K. Palanivelu, *J. Min. Mater. Charact. Eng*., **9**, 671 (2010).
17. F. Bensadoun, N. Kchit, C. Billotte, S. Bickerton, T. Francois and E. Ruiz, *Int. J. Polym. Sci*., Article ID 964193 (2011).
18. L.S. Schadler, In eds.: P.M. Ajayan, L.S. Schadler and P.V. Braun, Polymer-Based and Polymer-Filled Nanocomposites, Wiley-VCH Verlag, Weinheim, p. 77 (2003).
19. J. Choonghee and H.E. Naguib, *J. Cell Plast*., **43**, 111 (2007).
20. Q. Yuan and R.D.K. Misra, *J. Polym. Sci*., **47**, 4421 (2006).
21. K.H. Wang, M.H. Choi, C.M. Koo, Y.S. Choi and I.J. Chung, *Polymer*, **42**, 9819 (2001).
22. H. Khanjanzadeh, T. Tabarsa, A. Shakeri and A. Omidvar, *Wood Mater. Sci. Eng*., **6**, 207 (2011).
23. Y. Copur, C. Guler, C. Tascioglu and A. Tozluoglu, *Build. Environ*., **42**, 2568 (2006).
24. Y. Dong and D. Bhattacharyya, *Comp. A*, **39**, 1177 (2008).
25. S.C. Tjong, *Mater. Sci. Eng*., **53**, 73 (2006).
26. Y. Dong, D. Bhattacharyya and P.J. Hunter, *Comp. Sci. Technol*., **68**, 2864 (2008).
27. F.M.B. Coutinho, T.H.S. Costa and D.L. Carvalho, *J. Appl. Polym. Sci*., **65**, 1227 (1997).
28. Y. Zhao, K. Wang, F. Zhu, P. Xue and M. Jia, *Polym. Degrad. Stab*., **91**, 2874 (2006).
29. J. Jordan, K. Jacobb, R. Tannenbaumc, M. Sharafb and I. Jasiukd, *Mater. Sci. Eng. A*, **393**, 1 (2005).
30. K. Masenelli-Varlot, E. Reynaud, G. Vigier and J. Varlet, *J. Polym. Sci. B*, **40**, 272 (2002).
31. C.M. Chan, J. Wu, J. Li and Y. Cheung, *Polymer*, **43**, 2981 (2002).
32. F.H. Gojny, M.H.G. Wichmann, B. Fiedler, W. Bauhofer and K. Schulte, *Comp. A*, **36**, 1525 (2005).
33. A.H. Hemmasi, H. Khademi-Eslam, M. Talaiepoor, B. Kord and I. Ghasemi, *J. Reinf. Plast. Comp*., **29**, 964 (2010).
34. G. Han, Y. Lei, Q. Wu, Y. Kojima and S. Suzuki, *J. Polym. Environ*., **16**, 123 (2008).
35. S. Mohanty and S.K. Nayak, *J. Polym. Comp*., **28**, 153 (2007).
36. M. Razavi-Nouri, F.J. Dogouri, A. Oromiehie and A.E. Langroudi, *Iran. Polym. J*., **15**, 757 (2006).
37. I. Svab, V. Musil and M. Leskovac, *Acta Chim. Slov*., **52**, 264 (2005).